AGU PUBLICATIONS

Geochemistry, Geophysics, Geosystems

RESEARCH ARTICLE
10.1002/2017GC007175

Paleoproterozoic Geomagnetic Field Strength From the Avanavero Mafic Sills, Amazonian Craton, Brazil

A. Di Chiara[1,2], A. R. Muxworthy[3], R. I. F. Trindade[1], and F. Bispo-Santos[1]

[1]Departamento de Geofisica do Insituto de Astronomia Geofisica e Ciencias Atmosfericas, Universidade de São Paulo, IAG, São Paulo, Brazil, [2]Now at School of Geography, Earth and Environmental Sciences (SoGEES), Plymouth University, Plymouth, UK, [3]Department of Earth Science and Engineering, Natural Magnetism Group, Imperial College of London, London, UK

Key Points:
- We present some of the first paleointensity data from Precambrian South America using a multi-method approach
- The virtual dipole moments are $1.3 \pm 0.7 \times 10^{22}$Am^2 (Cotingo sill) of $2.0 \pm 0.4 \times 10^{22}$Am^2 Puiuà) and $6 \pm 4 \times 10^{22}$Am^2 (Pedra Preta)
- Results are comparable with contemporaneous data available from other regions

Supporting Information:
- Supporting Information S1

Correspondence to:
A. Di Chiara,
dichiaraanita@gmail.com

Citation:
Di Chiara, A., Muxworthy, A. R., Trindade, R. I. F., & Bispo-Santos, F. (2017). Paleoproterozoic geomagnetic field strength from the Avanavero mafic sills, Amazonian Craton, Brazil. *Geochemistry, Geophysics, Geosystems*, *18*, 3891–3903. https://doi.org/10.1002/2017GC007175

Received 7 AUG 2017
Accepted 24 SEP 2017
Accepted article online 29 SEP 2017
Published online 13 NOV 2017

Abstract A recent hypothesis has suggested that Earth's inner core nucleated during the Mesoproterozoic, as evidenced by a rapid increase in the paleointensity (ancient geomagnetic field intensity) record; however, paleointensity data during the Paleoproterozoic and Mesoproterozoic period are limited. To address this problem, we have determined paleointensity from samples from three Paleoproterozoic Avanavero mafic sills (Amazonian Craton, Brazil): Cotingo, 1,782 Ma, Puiuà, 1,788 Ma, and Pedra Preta, 1,795 Ma. We adopted a multiprotocol approach for paleointensity estimates combining Thellier-type IZZI and LTD-IZZI methods, and the nonheating Preisach protocol. We obtained an average VDM value of $1.3 \pm 0.7 \times 10^{22}$Am^2 (Cotingo) of $2.0 \pm 0.4 \times 10^{22}$Am^2 (Puiuà) and $6 \pm 4 \times 10^{22}$Am^2 (Pedra Preta); it is argued that the Cotingo estimate is the most robust. Our results are the first data from the upper Paleoproterozoic for South America and are comparable to data available from other regions and similar periods. The new data do not invalidate the hypothesis of that Earth's inner core nucleated during the Mesoproterozoic.

1. Introduction

The Precambrian geomagnetic field is poorly constrained despite this era covering >85% of Earth's history (Biggin et al., 2009). The knowledge of the Precambrian geomagnetic field is of vital importance to our understanding of the thermal evolution of Early Earth and inner-core formation. There are various models for inner-core nucleation (e.g., Aubert et al., 2009; Driscoll, 2016; Landeau et al., 2017; Ziegler & Stegman, 2013), which predict a minimum of ancient magnetic field intensity (paleointensity) followed by an abrupt increasing of strength. There are differences in the timing and size of this increase, depending on differing heat flows regimes at the CMB (Core Mantle Boundary) (e.g., Pozzo et al., 2012). The predicted timing of nucleation can be anywhere between ~1.8 and 0.6 Ga. Biggin et al. (2015) analyzed the Precambrian paleointensity database available (PINT15.05, Biggin et al., 2010) and hypothesized that after an early stage from 3.45 to 2.45 Ga of relatively high strength, the field strength decreased during a "Proterozoic dipole low," before increasing during the Mesoproterozoic. Biggin et al. (2015) linked this dipole low to inner-core nucleation; however, the current PINT2015 database (Biggin et al., 2010) is dominated by data obtained in Mesozoic and Cenozoic rocks from the northern hemisphere and likely does not capture the true field behavior; only 363 data are available (of which 43 were excluded for having a $Q_{PI} = 0$ (Quality criteria (Q_{PI}) as defined in Biggin & Paterson (2014)). However, Smirnov et al. (2016) argued that some of the high paleointensity values at ~1.2 Ga in the database are an artifact of the choice of low-temperature slopes in Arai plots. When these values are removed, the 1.2 Ga high ceases to exit and the paleointensity variations between 2 and 1 Ga fall within the range of the field in the last 20 million years (thus viewed as representative of natural typical variations in the presence of a solid inner core). Nevertheless, the current data set is insufficient in terms of dispersion and paucity to unequivocally resolve the question of the timing of inner core nucleation.

This dispersion and paucity of the paleointensity database is due to three main issues: (1) limitations of absolute paleointensity methods, (e.g., high-failure rates and time-consuming nature of experiments), (2) remagnetization processes (magnetic overprinting) that reduces the number of suitable targets (particularly true for ancient rocks), and (3) errors in age estimation, which for older rocks can be—in some cases—significant. Essentially, two main families of absolute paleointensity methods exist: heating and nonheating protocols. Most heating methods are based on the Coe (1967) modification of the Thellier and Thellier (1959) protocol,

consisting of the double heating of specimens under controlled laboratory magnetic field conditions, with various checks to test for nonideal behavior (e.g., Coe et al., 1978; Smirnov et al., 2003; Tauxe & Staudigel, 2004; Tauxe & Yamazaki, 2007). These methods are based on four main assumptions: (1) the natural remanent magnetization (NRM) is a thermoremanence (TRM) in origin, (2) a linear relationship exists between TRM intensity and magnetic field strength for Earth-size intensities, (3) the remanence carriers are magnetically single domain (SD) or SD-like in behavior, and (4) during laboratory experiments the ability of the sample to acquire thermal remanence is not altered (Tauxe & Yamazaki, 2007). Given the very specific characteristics of materials for Thellier-Thellier-Coe methods, suitable targets are rare and failure rates can be as high as 100%.

Some protocols have been developed to try to isolate the SD signal, including: (1) careful selection of material (eg., Pick & Tauxe, 1993), (2) careful preselection of samples (e.g., Valet et al., 2010), and (3) systematic low-temperature demagnetization (LTD) (e.g., Celino et al., 2007). However, these modifications still rely on multiple heating steps which can lead to chemical alternation during heating; chemical instability during heating in the laboratory is also a well-known issue that is identified through partial TRM (pTRM) checks (Coe et al., 1967). For example, Pick and Tauxe, 1993; Smirnov et al., 2003, for example, Thomas, 1993; Valet et al., 2010. Protocols with reduced heating steps (i.e., a reduction of the total number of heating steps or maximum temperature) do exist, (i.e., a reduction of the total number of heating steps or maximum temperature), such as the Shaw (Shaw, 1974) method, the microwave method (Walton et al., 1993), the Wilson method (Muxworthy, 2010), and the multispecimen parallel differential partial-TRM (pTRM) method (Dekkers & Böhnel, 2006). These methods are expected to suffer less from the effects of chemical alteration, but are not immune because they all still involve some sample heating. To completely remove the effects of chemical alteration during laboratory heating various nonheating methods have been developed. They comprise of the "REM-type" protocol (Gattacceca & Rochette, 2004; Kletetschka et al., 2000) and the Preisach protocol (Muxworthy et al., 2011a; Muxworthy & Heslop, 2011). REM-type methods are currently the most commonly used nonheating method such as the pseudo-Thellier (de Groot et al., 2013; Paterson et al., 2016); they essentially provide a calibrated measurement of relative intensity, based on normalization by isothermal remanent magnetization (IRM). In contrast, the Preisach paleointensity protocol is a first-principles, first-order method.

There is clearly a need for more robust paleointensity estimates from well-dated Precambrian rocks from the southern and low latitudes. Here, we report new absolute paleointensity data for well-dated samples from Avanavero, Amazonian Craton, Brazil. The Avanavero magmatic suite has been zircon dated by U-Pb SHRIMP to 1,788.5 $\pm$ 2.5 Ma (Santos et al., 2003), which has been averaged between six geochronological ages from different levels of sills and dykes: ranging from 1,973 $\pm$ 2 to 1,795 $\pm$ 2 Ma. These rocks were originally sampled by Bispo-Santos et al. (2014), who conducted a standard palaeomagnetic paleogeographic study using thermal and alternating-field (AF) demagnetization data. Their study identified a clear characteristic remanent magnetization (ChRM), whose primary remanence was verified by a positive baked-contact test. Assuming that the field was essentially dipolar during that time period, the Avanavero sills were emplaced between 20°S and 6°N paleolatitude (Bispo-Santos et al., 2014). Rock magnetic analysis by Bispo-Santos et al. (2014) suggests that the ChRM is carried by Ti-poor titanomagnetite with moderate to high coercivity (H_C) and high unblocking temperatures (T_{UB}). Although the Thellier-Thellier-Coe protocol is the generally accepted method for paleointensity determination, it is still prone to errors, and many tests have been performed in order to identify the best overall method without clear consensus. To accommodate this, it has been suggested that multiprotocol paleointensity studies may obtain the most robust paleointensity estimates through interprotocol coherence (e.g., Muxworthy et al., 2011b). In this way, we opt in the present study for a multiprotocol approach in order to determine robust absolute paleointensity estimates from Paleoproterozoic dykes from the Avanavero sample collection. As it is seen in this paper, many of our samples displayed chemical alteration during heating; in our multiprotocol approach, we consider both heating and nonheating paleointensity approaches.

2. Methods and Analyses

2.1. Geological Setting

The study area is part of the oldest portion of the Amazonian Craton (>2,600 Ma), which is one of Earth's largest stable areas (430,000 km^2). It is formed by two sectors—the northern Guiana Shield and the southern Central-Brazil or Guaporé Shield—separated by the Phanerozoic Amazonian sedimentary basin

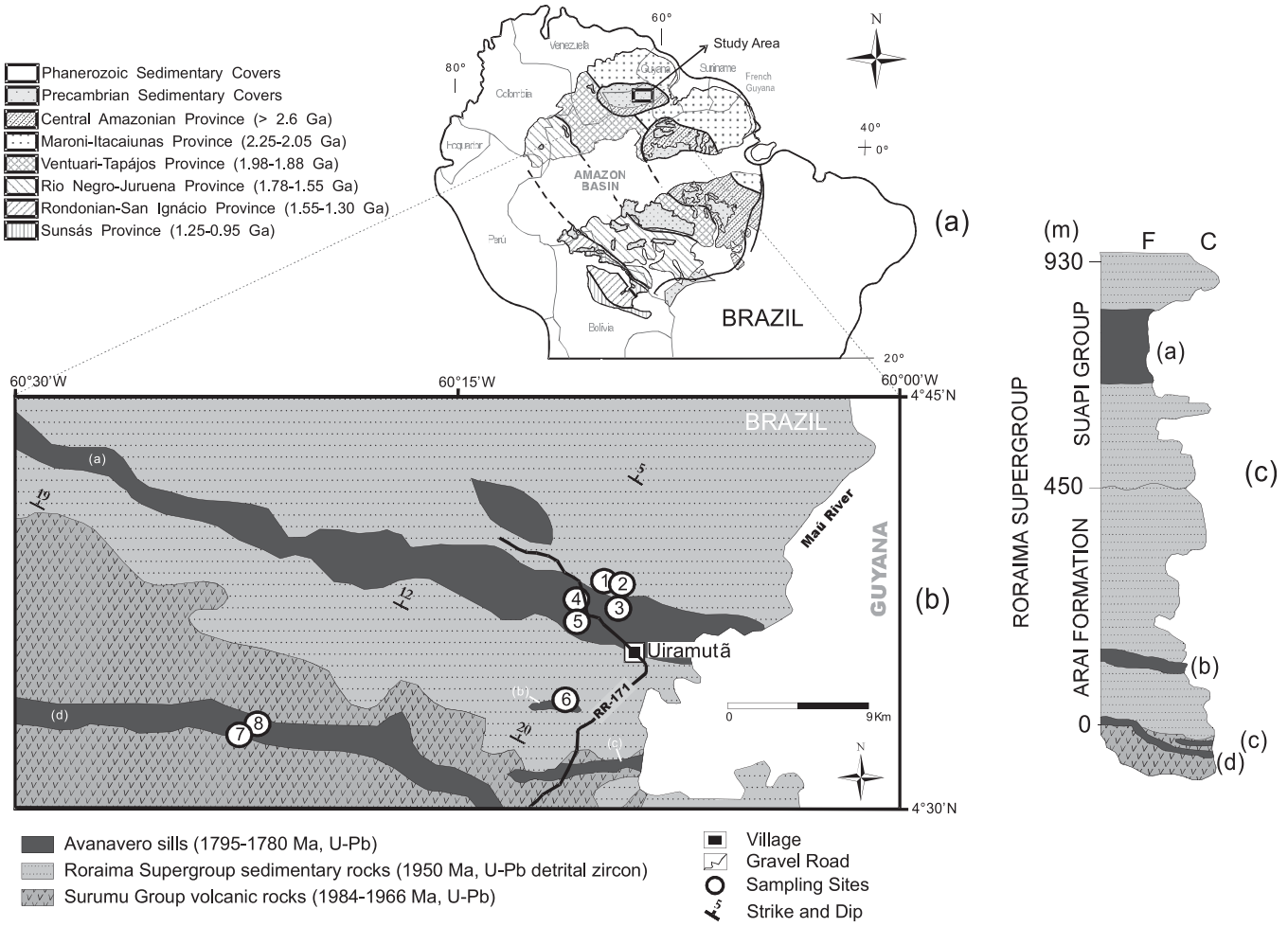

Figure 1. Geological map of the studied area and location of the sampling sites, modified after Bispo-Santos et al. (2014). The Avanavero sills are marked in black where: (a) is the Pedra Preta, (b) Puiuà, (c) Camararem, and (d) Cotingo. Sampled sites are marked from 1 to 5 (FR1 to FR5), 6 (FR11), and 7 and 8 are (FR143 to 145). The inset represents Amazonian Craton and their geochronological Provinces.

(Lacerda-Filho et al., 2004). The Maroni-Itacaiúnas Province is in the northeastern part of the Amazonian Craton and is dominated by two Hadean-Archean cores (one of which the central Amazonian province, CAP > 2,600 Ma, in Figure 1a) surrounded by a predominantly accretionary Paleoproterozoic belt (2,250–2,050 Ma) (Tassinari & Macambira, 1999), while the southwestern part of the Hadean-Archean core was accreted by subduction-related juvenile magmatic arcs forming the Ventuari-Tapajós (1,980–1,810 Ma) and the Rio Negro-Juruena (1,780–1,600 Ma) Provinces.

The samples in this paper are from the Avanavero magmatic event, part of the CAP known as the Roraima block. They were collected and reported by Bispo-Santos et al. (2014). The Roraima block is covered by the 1,980–1,960 Ma Sumuru acid volcanic rocks and by the ~1,870 Ma sedimentary Roraima Supergroup Formation (Figure 1c) (Santos et al., 2003; Tassinari & Macambira, 1999). The Avanavero volcanic event, with mafic sills and dykes, intruded both the Surumu Group volcanic and the Roraima Supergroup (Reis et al., 2013), extending to Venezuela, Guyana, and Suriname (they form a large igneous province, LIP). The sills followed the original structures of the Roraima sedimentary rocks, that is, their bedding planes striking NW-SE and dipping 5–20°. The Avanavero suite sampled in Brazil comprises four levels of sills from the Late Paleoproterozoic (Statherian period) informally called: Cotingo (dolerite 40 m thick, dated 1,782 ± 3 Ma with U-Pb, Santos et al., 2003), Camararém, Puiuà (20 m thick), and Pedra Preta (250 m thick) (dated to 1,795 ± 2 Ma with U-Pb baddeleyite age, Reis et al., 2013) (Figure 1). An average dating for the Avanavero intrusive event of 1,788.5 ± 2.5 Ma (Bispo-Santos et al., 2014) was used for the Puiuà sill where no direct dating was made.

Table 1
Site Location and Previous Paleomagnetic Directional Results From Bispo-Santos et al. (2014)

Site	Lat (S)	Lon (W)	Age (Ma)	*n/N*	*D* (°)	*I* (°)	α_{95} (°)	Paleolatitude (°)
Pedra Preta								
FR01	04°37.8′	60°09.6′	1795 ± 2	15/15	141	13	4	6
FR02	04°37.8′	60°09.6′		16/16	140	12	4	6
FR03	04°37.2′	60°09.6′		12/13	136	13	5	6
FR04	04°37.2′	60°10.2′		12/12	140	−7	3	−4
FR05	04°36.6′	60°10.2′		12/17	103	−14	3	−7
Puiuà								
FR11	04°34.2′	60°11.4′	1788.5 ± 2.5	18/13	151	27	5	14
Cotingo								
FR143	04°32.4′	60°19.8′	1782 ± 3	12/12	157	−37	3	−21
FR144	04°32.4′	60°19.8′		14/14	147	−22	2	−11
FR145	04°32.4′	60°19.8′		5/13	115	11	9	6

Note. Unit names given in italics. n/N is the number of determined directions and the number of samples measured, D is the declination, I the inclination, and α_{95} the confidence limit on the direction.

In the present study, we selected five sites (FR1–FR5) from Pedra Preta sill, one site (FR11) from Puiuà and three sites (FR143–FR145) from the Cotingo dolerite sill (Table 1). The Avanavero rocks comprise dark-gray medium to coarse-grained dolerites and gabbros, and subordinate microdiorites and microquartz diorites (Reis et al., 2013). An optical microscope investigation (supporting information) reveals that they are composed of plagioclase, pyroxene, and amphibole, with magnetite and ilmenite as accessory minerals. Dolerite dykes show generally subophitic texture, and are composed of plagioclase (labradorite), pyroxene (augite and occasionally pigeonite), and hornblende. Sericite, chlorite, and epidote appear as accessory minerals (Reis et al., 2013) for late hydrothermal processes (such as alteration of plagioclase), however Bispo-Santos et al. (2014) performed a baked contact test, which rules out regional remagnetization.

2.2. Paleointensity Analyses

On the Avanavero sample collection (Bispo-Santos et al., 2014) we applied three absolute paleointensity methods: two Thellier-type protocols (IZZI and LTD-IZZI) and the nonheating Preisach protocol. To select the samples for paleointensity investigations, a preliminary rock-magnetic screening study was conducted. Following Valet et al. (2010), we selected samples: (1) with no evidence of multiple magnetizations, i.e., near "univectorial" behavior, (2) displaying reversible features on high-temperature susceptibility-temperature curves, and a "single" Curie temperature, and (3) a predominately SD-like (or nonmultidomain-like) signal in hysteresis curves. From about 250 samples available, only 95 samples met these preselection criteria and were subjected to paleointensity experiments (Figure1 and Table 1). Five thin sections from sites FR1, FR2, FR3, and FR5 were examined in the optical microscope (supporting information), to determine magnetic minerals' alteration states (Haggerty, 1991).

A first batch of samples was measured with the IZZI protocol (Tauxe & Staudigel, 2004). Four to six fresh specimens were chosen from each unit. A total of 40 specimens corresponding to small rock chips (<5 g) were placed in clean glass vials and fixed with microfiber glass filters and Kasil glue in order to minimize the contact with air. A laboratory field (25 μT) was applied along the samples' core axis. PTRM checks (Coe, 1967) were made every two steps to check for laboratory chemical alteration. Each specimen was treated with a total of 32 heating steps, in 100°C intervals up to 300°C, 50°C intervals up to 500°C, and 10°C intervals up to 600°C. Heating/cooling cycles were performed in TD48SC furnace (ASC Scientific), and the remanence measured using a long-core 755 2G SQUID magnetometer housed in a magnetically shielded room (ambient field < 500 nT) at the Laboratorio de Paleomagnetismo of Universidade de São Paulo (Brazil).

A second batch of samples was measured using the LTD-IZZI protocol (e.g., Yamamoto et al., 2003): Liquid nitrogen pretreatment after every heating step (low-temperature demagnetization for 20–30 min) was incorporated in the protocol to reduce the effects of multidomain (MD) grains (e.g. Celino et al., 2007). During zero-field cooling through the Verwey transition (∼125 K), remanence carried by MD grains is thought to be preferentially removed, thus enhancing SD-like remanence. Because of their unstable behavior in the first set of experiments, samples from three of nine studied sites were excluded from the second set of

experiments. A total of 43 minicore specimens (9.8 cm^3) were prepared from the remaining six sites. A laboratory field of 25 μT was chosen and the specimens were subjected to 47 heating steps from 20 to 580°C.

Because of strong evidence for chemical alteration of several samples during heating, a third batch of experiments was run using a nonheating Preisach paleointensity protocol (Muxworthy & Heslop, 2011). The protocol includes theoretical features not accommodated by previous nonheating paleointensity methods. For example, it includes magnetostatic interactions, allows for variable cooling rates, and can identify, isolate, and reject unstable remanence carriers, that is, MD and superparamagnetic contributions. Instead of measuring a rock's response to TRM acquisition in a laboratory field as in Thellier-type methods, the Preisach-based approach predicts the high-temperature behavior of magnetic particles in a sample from their Preisach distribution (Preisach, 1935) obtained at room temperature from first-order reversal curve (FORC) data (Roberts et al., 2000). The paleointensity estimate is determined by comparing the AF demagnetization spectra of the sample's natural remanent magnetization and a simulated TRM. The data are normalized by the saturation isothermal remanent magnetization (SIRM) AF demagnetization curve. In contrast to the original protocol, where normalization is undertaken by a single SIRM measurement, in this paper we use SIRM AF demagnetization spectra. To test for the robustness of the Preisach model, we compare the measured and predicted SIRM AF demagnetization spectra and have introduced new additional selection criteria: the "plateau Preisach paleointensity protocol" (supporting information). This updated Preisach protocol was applied to 28 cylindrical minispecimens (∼1 cm^3). Samples were AF demagnetized using a Molspin tumbling AF demagnetizer with 14 demagnetization steps from 0 to 100 mT and remanent magnetization was measured with an Agico JR-5 spinner magnetometer at Imperial College London. SIRM AF demagnetization spectra were measured by applying a 1 T pulse field (ASC Scientific Pulse Magnetizer).

Hysteresis, back-field curves, and FORC data were measured using a Princeton Instruments Vibrating Sample Magnetometer (VSM) at Imperial College London. The magnetic mineralogy was determined from high-temperature susceptibility curves measured on one or two specimens per site in order to investigate the distribution of Curie temperatures and the thermal reversibility using a CS-4 apparatus coupled to the KLY-4S Kappabridge instrument (Agico) at Universidade de São Paulo.

3. Results

3.1. Magnetic Mineralogy and Domain State

Generally, the high-temperature susceptibility shows Hopkinson peaks and Curie temperatures ∼580°C indicating the presence of low-Ti titanomagnetite (Figure 2 and supporting information). Three different behaviors were classified: group 1 (Figure 2a), with multiple Curie temperatures indicating the presence of Ti-rich iron oxide phases and possible maghemite in the samples (possible inversion temperature at ∼350°C), plus a Ti-poor titanomagnetite 580°C phase and a small hematite-like phase at ∼680°C; the curves were not entirely reversible. Group 2 (Figures 2b and 2c) display a clear Curie temperature near 580°C, with evidence for the inversion of a maghemite-like phase between 300 and 500°C on heating; this inversion leads to a drop in the susceptibility on the reverse cooling curve. Group 3 has an almost reversible heating and cooling curve, with a Curie temperature at ∼585°C (Figure 2d).

T, the standard hysteresis parameters were determined through hysteresis measurements: saturation magnetization (M_S), remanent saturation magnetization (M_{RS}), coercivity (H_C), and the remanent coercivity (H_{CR}). Ratios of these parameters are plotted on in Figure 3 Most of the specimens show hysteresis parameters in the central region of the plot indicating a moderately stable magnetic carriers (Figure 3). Noticeably, the specimens' domain states from the same site were fairly consistent.

Typical FORC diagrams are shown in Figure 4. The FORC diagrams fell into essentially two types of behavior: (1) these FORC distributions displayed distinct peaks (peak coercivity values were ∼ 20 mT), with the distribution extended along the H_C-axis with little spreading in the H_u-axis direction, suggesting the presence of noninteracting SD grains (units FR1, FR2, and FR3 only; Figures 4a and 4b), and (2) these FORC diagrams displayed a more "MD-like" (Muxworthy & Dunlop, 2002), but with narrow high-coercivity, SD-like tails (Figure 4c and 4d).

Optical microscopy revealed iron oxide grains tens of microns in size, with well-developed oxyexsolution lamellae, corresponding to oxidation class C4 to C6 of Haggerty (1991). Some grains were smaller with little sign of oxidation (class C2) (see supporting information).

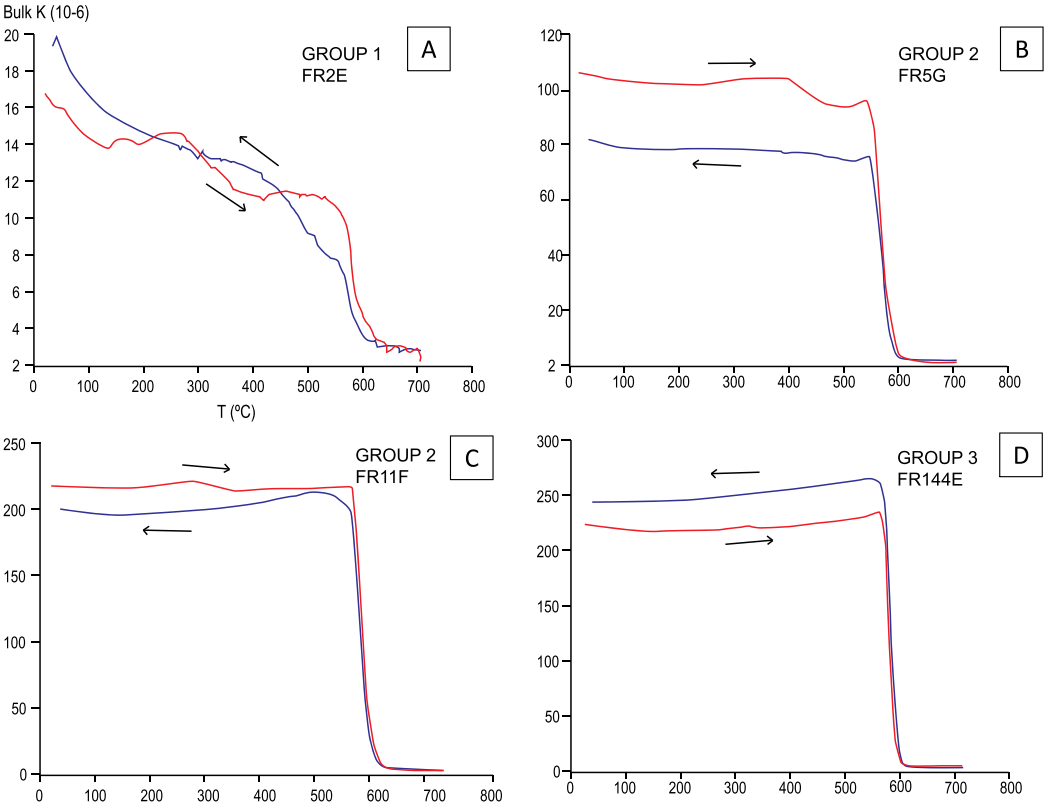

Figure 2. Example thermomagnetic curves showing variation in magnetic susceptibility K (SI) versus high and low temperature (curves were corrected from furnace effects): (a) Group 1 behavior (sample FR2E), (b) Group 2 behavior (sample FR5G), (c) Group 3 behavior (sample FR11F), and (d) Group 4 behavior (sample FR144E).

3.2. Paleointensity Results

Representative results from the IZZI and IZZI-LTD experiments are shown in Figure 5. In most of the cases, the magnetization unblocked above 520°C suggesting that the NRM is dominated by SD or small magnetite grains. The thermal data were analyzed with Thellier_GUI program (Shaar & Tauxe, 2013), and the paleointensity estimates are summarized in Table 2; data at the specimen level are reported in the supporting information (Tables S2 and S3). In order to select reliable estimates, we used the TTB cutoff criteria as defined by Paterson et al. (2014). We did not make pTRM-tail checks; therefore, the following criteria were used: at specimen level a minimum of five steps (n), $f \geq 0.35$, $q \geq 0$, $\beta \leq 0.15$, an anchored mean angular deviation $MAD_{anc} \leq 15°$, $\alpha \leq 15°$, $\delta CK \leq 9\%$ and $\delta pal \leq 18\%$; see the supporting information and Paterson et al. (2014) for a full definition of these parameters.

Specimens exhibit a variety of behaviors in the Arai plots (Figure 5): (1) segmented, with two different slope angles often between 450 and 525°C (Figure 5a), (2) zigzagged, typical for MD behavior in IZZI-type protocols, (3) curved (Figures 5c and 5e), and (4) some were too scattered to plot displaying erratic behavior. The last case occurred when no straight line could be plotted or specimens did not acquire any laboratory TRM. While many samples displayed apparently unstable low-temperature Arai segments and were rejected, the paleointensity estimates were taken from high-temperature segments that passed the selection criteria (see supporting information Tables S2 and S3).

From the IZZI experiments, 10 specimens of the 42 analyzed passed the selection criteria (Table 2, supporting information Table S2) with a specimen level success rate of 24%; four out of nine analyzed sites gave paleointensity results from two or more specimens (FR1, FR2, FR3, and FR144). From the LTD-IZZI experiments, three specimens of the 44 analyzed passed the selection criteria (~7% success rate) from one of the six sites investigated (FR144, Table 2 and supporting information Table S3). From the Preisach protocol, 6 of the 26 specimens analyzed gave yielded estimates (a ~23% success rate at specimen level). Specimens were rejected if the simulated and measured SIRM AF demagnetization curves differ significantly

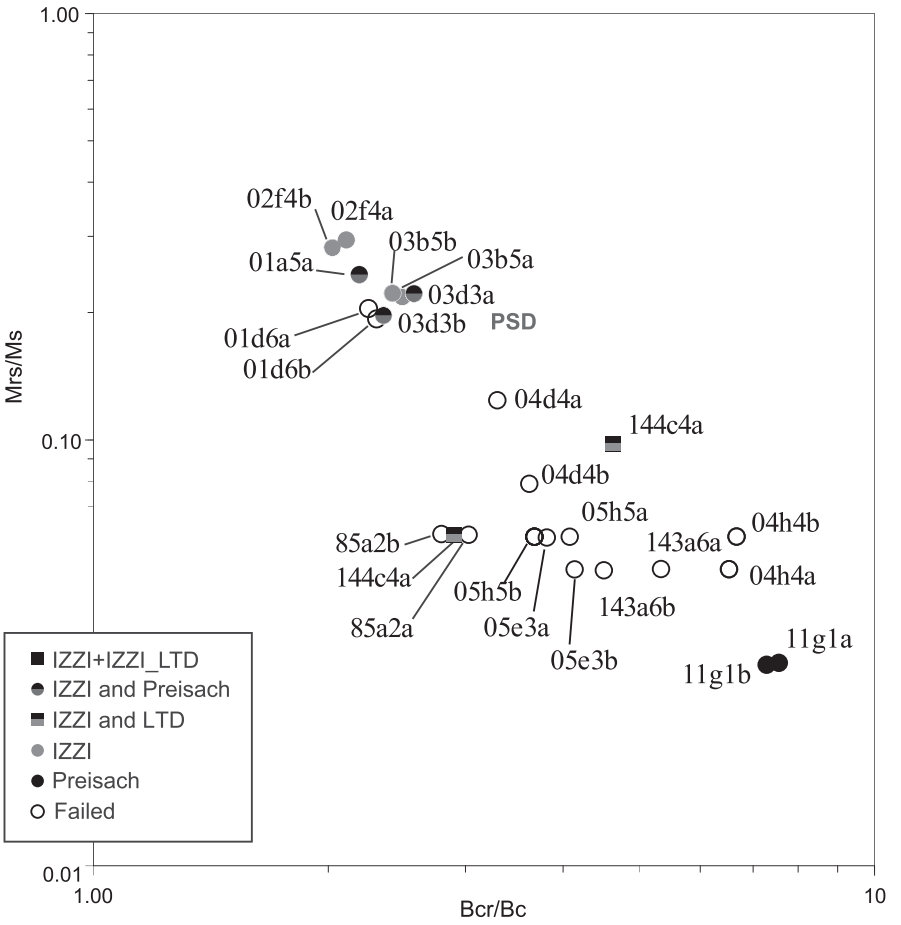

Figure 3. Logarithmic plot of hysteresis ratios M_{RS}/M_S versus B_{CR}/B_C. Data points are specimens from the Avanavero samples collection (label FR- is omitted) and symbols correspond to method(s) which gave reliable paleointensity results. The regions commonly associated with SD, PSD, and MD behaviors are labeled. For clarity in the figure, "FR" is removed from the sample names. Specimen data are given in supporting information Table S1.

(supporting information Table S4). Most samples did not meet the Preisach paleointensity acceptance criteria (see supporting information). The site that displayed the clearest plateau behavior was the FR11 (see supporting information). Sites FR1 and FR3 had less well-defined plateaux, and gave high estimates compared to the thermal methods, raising questions on the reliability of the identification of these plateaux (especially for site FR1). Samples from FR4 and FR5 had very high NRM/SIRM ratios (6–18%), which are indicative of NRMs with a chemical rather than thermal origin, which could be caused by lightning strikes.

4. Discussion

At specimen level the success rates of the IZZI, LTD, and Preisach experiments were low at approximately 24%, 7%, and 23%, respectively (Table 2, supporting information). The high failure rates of the heating experiments can be partially explained in two ways: (1) thermal instability of the samples, (2) a high-proportion of MD grains; both of these effects were minimized by using the Preisach method. Chemical alteration during heating was monitored with pTRM checks and samples rejected accordingly. Additionally, the high NRM/SIRM ratios identified in some of the samples, suggested that not all the NRMs were TRMs, a requirement for all the paleointensity methods used in this study; this also led to failure of some paleointensity experiments.

There does not appear to be a clear correlation between domain state and paleointensity success (Figure 3), in agreement with Carvallo et al. (2006). For example, of the four FORC diagrams (Figure 4), the presence of noninteracting SD grains (Figures 4a and 4b) or more MD-like diagrams (Figures 4c and 4d) does not

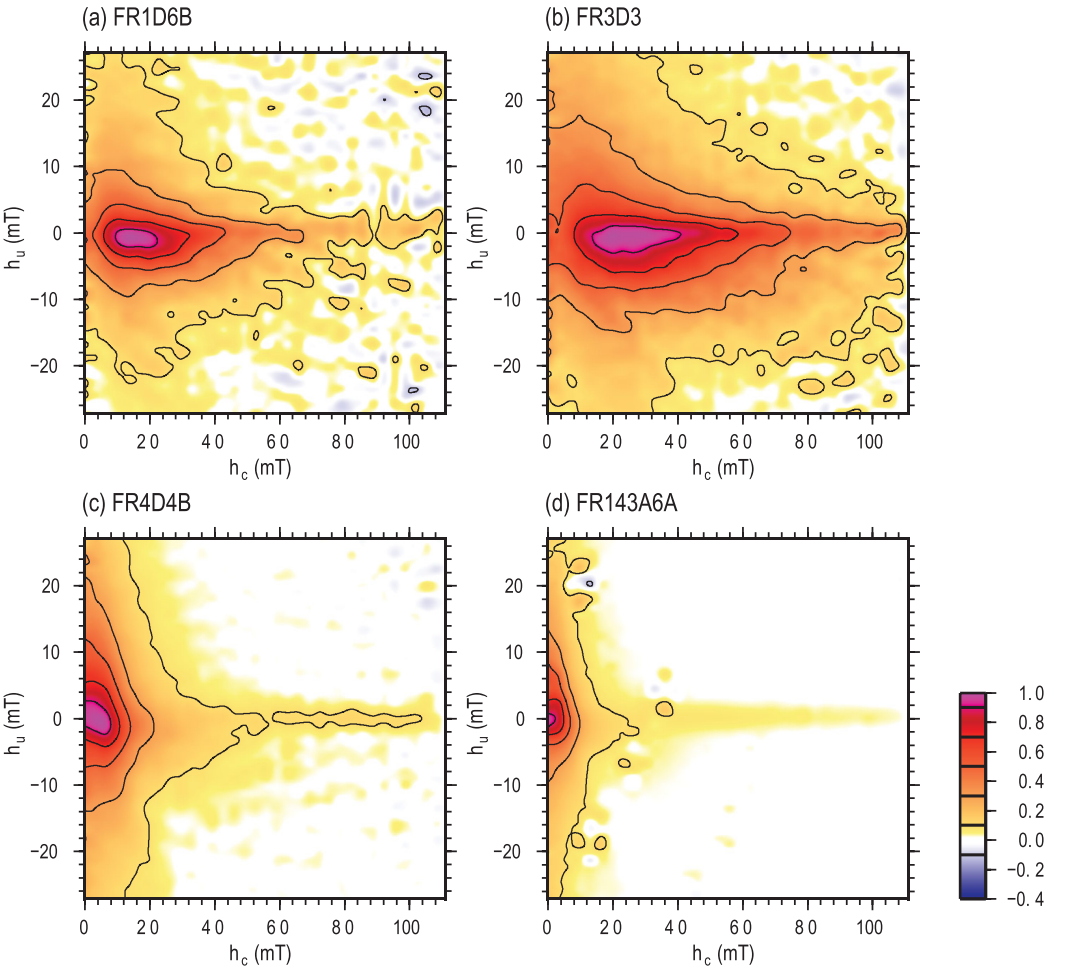

Figure 4. Normalized FORC diagrams for samples (a) FR1D6, (b) FR3D3, (c) FR4D4, and (d) FR143A6A. Smoothing factor is 3 in all the diagrams, and measurement time was 100 ms.

seem to influence the success or failure of our analyses. Optical microscopy (supporting information) found some (nonsystematic) evidence for oxyexsolution of MD or PSD magnetite formed possibly below the Curie temperature of magnetite, which could lead to lower paleointensity estimates (Smirnov & Tarduno 2005). The cooling rate might also have an effect on the paleointensity estimates. Given that most of the samples have a predominance of PSD grains, the effect could be up to the ∼10–15% (Biggin et al., 2013). On the Preisach method variations in cooling time (1 day to 10 kyr) made a negligible difference of < 1 μT to the final intensities, while further tests will be necessary to evaluate the effect on the results obtained with the IZZI and LTD methods. At this stage, we may suggest that such differences in cooling times could explain the low heating protocol results of all Pedra Preta sites when compared with the Preisach results. At the site level, the paleointensity results varied between methods (Table 2). Only the heating methods succeeded in providing estimates for sites FR2, FR144, and FR145, while for site FR11 only the Preisach method provided a result. Generally, the LTD-IZZI method was used to minimize the MD grains contribution, and the Preisach approach to reduce the effect of chemical alteration. When the nonheating Preisach-based protocol was applied, we obtained higher values with respect to the heating protocols results (FR1 and FR3), possibly due to low-temperature alterations in the heating results. The IZZI protocols produced very similar paleointensity estimates to the LTD-IZZI for site FR144 (Table 2).

Simple thermal conduction models (Jaeger, 1968) estimate that the time of cooling of igneous intrusions depends on the square of the half-thickness of the intrusion. For the Avanavero sills, the complete cooling of the intrusions could be of ∼100 years for Puiuà and Cotingo, and 5,000 years for Pedra Preta. Due to the slow cooling rates, we can consider that the secular variation has been averaged. Hence, our low intensity

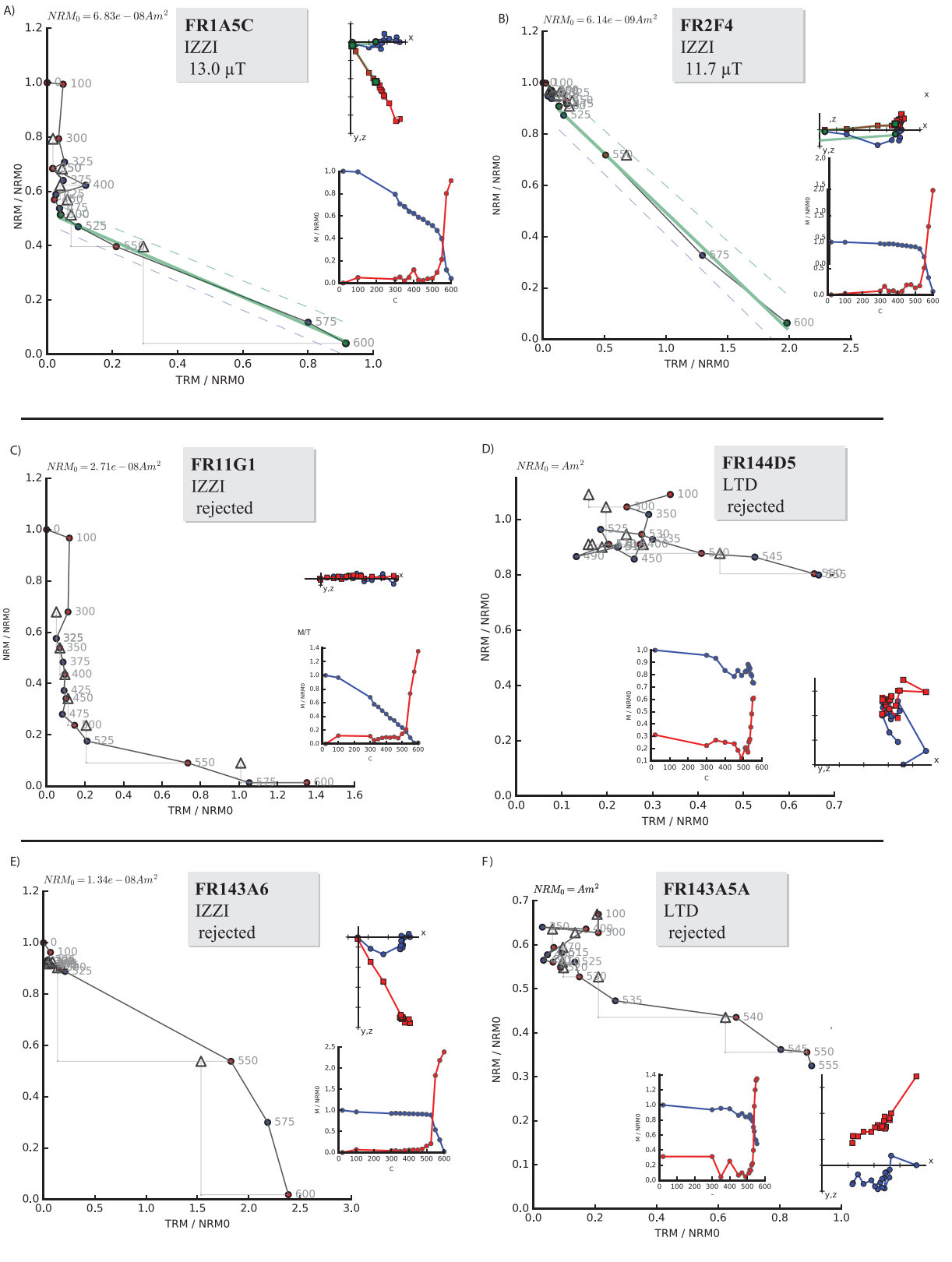

Figure 5. Six representative Arai plots from IZZI Thellier and LTD Thellier paleointensity results. The inset figure to the upper right of each diagram illustrates the demagnetization behavior of the specimen on a vector component plot and on the lower right plot is the original magnetization lost (NRM in blue) and acquired (pTRM in red) during the procedure.

Table 2
Summary of the Paleointensity Results

	IZZI			LTD-IZZI			Preisach		
Site	*n/N*	B (μT)	VDM	*n/N*	B (μT)	VDM	*n/N*	B (μT)	VDM
Pedra Preta									
FR1	2/6	12 ± 1	3.1 ± 0.2	0/6	...	...	2/4	52 ± 6	16 ± 1
FR2	2/6	12 ± 1	3.0 ± 0.1	0/8	...	...	0/2	...	...
FR3	2/5	8 ± 2	1.9 ± 0.5	...	...	...	2/4	24 ± 2	6.2 ± 0.5
FR4	0/6	...	...	...	...	...	0/4	...	...
FR5	0/6	...	...	0/7	...	...	0/4	...	...
Puiuà									
FR11	0/6	...	...	0/7	...	...	2/2	8 ± 2	2.0 ± 0.4
Cotingo									
FR143	0/6	...	...	0/8	...	...	0/2	...	...
FR144	3/4	5 ± 2	1.1 ± 0.5	3/8	6 ± 1	1.6 ± 0.1	0/2	...	...
FR145	1/2	1	0.3	...	...	...	0/2	...	...

Note. n/N is the number of determined estimates and the number of samples measured, B the paleointensity and VDM the Virtual Dipole Moment (units are $10^{22}Am^2$). Standard deviations are given as error estimates. For site FR145 only one estimate was made; no standard deviation estimate is given. For specimen level results see the supporting information.

estimates cannot be ascribed to secular variations; also, the angular dispersion of the paleodirections of 18° (see Table 1 and discussion in Bispo-Santos et al., 2014) is compatible with that obtained with adequate sampling, thus averaging out the secular variations. Additionally, the Avanavero paleomagnetic directions (Table 1) were very similar to those found for Aro and Guaniamo dykes in Venezuela (600 km of distance; dated 1,820 Ma), suggesting that no significant tilting affected the region.

4.1. Comparison With the PINT Database

We plot the paleointensity data available for the Precambrian (650–4,000 Ma) from the PINT2015.05 database (Biggin et al., 2010) in Figure 6. We use the samples' quality values (Q_{PI}) (Biggin et al., 2015) scores to make two groups: one with $Q_{PI} > 1$, and another more exclusive one with $Q_{PI} > 3$ (320 estimates from 36 different studies). VDMs range from 1 to 14 × $10^{22}Am^2$, and many of the data sets have large dispersions, e.g., data from Canada. The Precambrian database shows two clusters of data in the Proterozoic between approximately 1.0 and 1.3 Ga, and 1.8–1.9 Ga. Geographically, the majority of the entries are from Canada, United States, Russia, Greenland, and Australia (Figure 6). The data set of South America is limited to one from the 1.2 Ga Nova Floresta Formation (Amazonian Craton, Brazil) by Celino et al. (2007) who used an LDT-Thellier protocol. Celino et al. (2007) obtained a VDM of 2.1 × $10^{22}Am^2$, which is similar to Canadian units of approximately the same age (Figure 6).

To compare our data with published data sets, we calculated the virtual dipole moment (VDM, Table 2) using the paleomagnetic inclinations obtained by Bispo-Santos et al. (2014) (Table 1, Figure 6c). We average estimates from all three methods (Table 2) for the three Avanavero sills: 1.3 ± 0.7 × $10^{22}Am^2$ for Cotingo (N = 2), 2.0 ± 0.4 × $10^{22}Am^2$ for Puiuà (N = 1), and 6 ± 4 × $10^{22}Am^2$ (N = 3; IZZI only, 2.7 ± 0.6 × $10^{22}Am^2$) from Pedra Preta using data from all the paleointensity methods (Figure 6). The VDM for Pedra Preta is heavily biased by the two Preisach FR1 estimates (Table 1), and displays large interprotocol variance; the value for Puiuà was from one method; consequently, the value for Cotingo is not only the lowest of the three but the most robust as it is displays interprotocol consistency.

We compare these three estimates to temporally "close" estimates, (i.e., +/–300 Ma; inset Figure 6b) from Sweden (Donadini et al., 2011; Elming et al., 2009), Canada (Kobayashi 1968; Schwarz & Symons, 1969, 1970), Siberia (Shcherbakova et al., 2006), and South Africa (Shcherbakova et al., 2014). Our VDM from Cotingo (1,782 Ma) is comparable to the coeval data from Sweden (Donadini et al., 2011), and younger data from Sweden and Russia (both younger by ~150 Ma). The Cotingo VDM estimate is lower than the slightly older estimates from Siberia (Schwarz & Symons, 1969; Shcherbakova et al., 2006), and from Canada (Kobayashi, 1968; Schwarz & Symons, 1970). Our Puiuà estimate (1,788 Ma), although less robust, fits the VDM

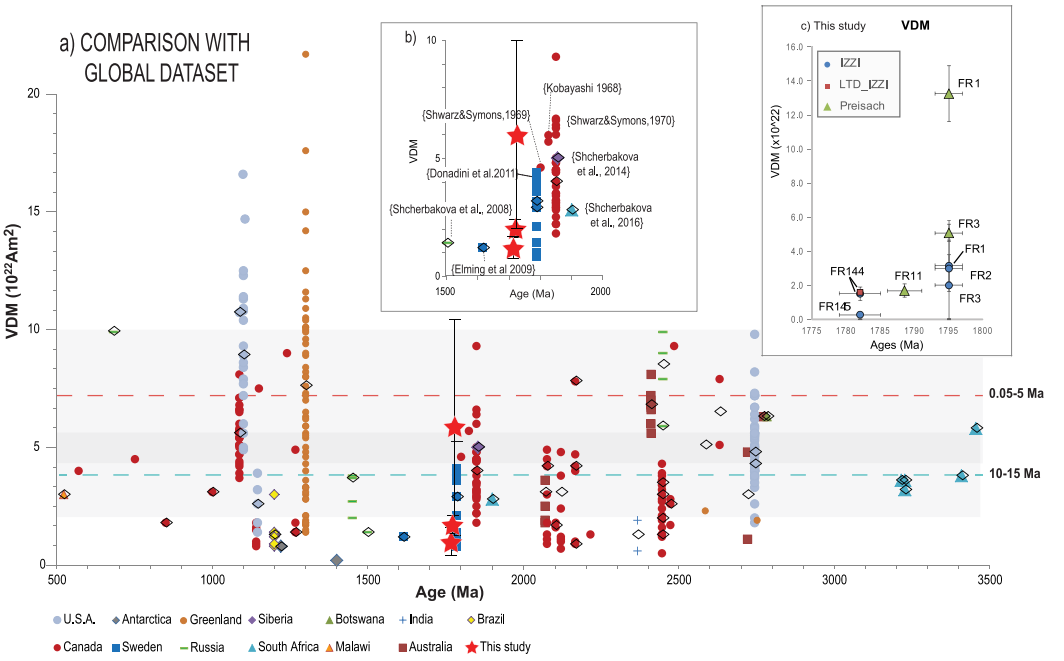

Figure 6. Comparison of data from this study (red stars) and data from the global data set of PINT2015.05 (Biggin et al., 2010) queried from 500 to 3.5 Ga, of which only data with a QPI >1 are shown (Biggin & Paterson, 2014). Empty diamonds symbols highlight data with a QPI >3 (Biggin et al., 2015). In inset (b) represents a detail of the comparison of our data and other data set within 300 Ma from different studies (references in brackets), inset (c) an overview of all the paleointensity results averaged per site obtained in this study using the three methods. Dashed lines represent mean paleointensity values for the 0.05–5 Ma and 10–15 Ma with uncertainties ($+/-1\sigma$) shown.

trend (Figure 6b). The Pedra Preta estimate (1,795 Ma) is higher than our two younger estimates, but, despite its large error, it is comparable with the high estimates from Canada (Kobayashi, 1968; Schwarz & Symons, 1970). If only the value obtained with the heating protocol is considered (IZZI only, $2.7 \pm 0.6 \times 10^{22}$Am^2), our value from Pedra Preta is similar to the Swedish (Donadini et al., 2011) and South African data (Shcherbakova et al., 2014), and lower than the older estimates from Canada and Siberia (Shcherbakova et al., 2014) and similar to our slightly younger value from Puiuà.

Our new data therefore support existing data trends (Figure 6), in particular the hypothesis of Biggin et al. (2015) of inner-core nucleation timing, between 2.4 and 1.3 Ga (midstage) supported by reduced VDM during this period. The gradual decrease during the midstage (Biggin et al., 2015) corresponds to a decreasing power of thermal convection due to the progressive cooling of the core (Aubert et al., 2010). The change around $\sim$1.3 Ga is interpreted as the timing of inner core nucleation. The data in this study is consistent with the low-field period, but they only cover a limited period of time (13 Myr).

If we consider the field variation during the entire Precambrian using the data with a $Q_{PI} \geq 3$ (Biggin et al., 2015) and compare the variation for the 0.05–5 Ma interval and 10–15 Ma, we observe similar fluctuations in field intensity (Figure 6a, as in Smirnov et al., 2016), but with lower mean values. This observation suggests that the hypothesis of the subdivision of the Precambrian in three intervals (as in Ziegler & Stegman, 2013, and in Biggin et al., 2015) could be also biased by the overall scarcity of data, which our data help to fill (Figure 6).

5. Conclusions

We present new paleointensity data from three Mesoproterozoic sills (Cotigo, 1,782 Ma, Puiuà, 1,788 Ma, and Pedra Preta, 1,795 Ma) sampled within the Avanavero magmatic intrusive suite in the NW of the Amazonian Craton (Brazil). Along with previous data from Celino et al. (2007), our results represent the only data from the South America for the Precambrian. The Avanavero suite had been previously shown to have the

potential to yield paleointensity values (Bispo-Santos et al., 2014), who ruled out regional remagnetization overprints with a positive contact test.

Using a multiprotocol paleointensity approach (IZZI, LTD-IZZI, and Preisach protocols), we obtained mean VDM values of $1.3 \pm 0.7 \times 10^{22}$Am^2 for Cotingo, $2.0 \pm 0.4 \times 10^{22}$Am^2 for Puiuà, and $6 \pm 4 \times 10^{22}$Am^2 (IZZI only, $2.7 \pm 0.6 \times 10^{22}$Am^2) from Pedra Preta; it is argued that the estimates for Cotingo are the most robust. The values are consistent with a period of low intensities (such as the midstage interval proposed by Biggin et al. (2015)). Our data alone do not confirm the hypothesis that Earth's inner core nucleated later during the Mesoproterozoic, but they do not nullify the hypothesis. Additional paleointensity data from Precambrian are needed to robustly verify this theory and understand the nature and evolution of Earth's early magnetic field.

Acknowledgment
This work was funded by FAPESP project 2013/08938-8, 2016/06114-6 and research scholarship (BEPE) granted by FAPESP (2014/19509-3) to A.D.C. Thanks to Daniele Brandth, Plinio Jaqueto, and Giovanni Moreira for the support in the laboratory of USP. Liliane Janikian provided the optical images in the supporting information section.

References

Aubert, J., Labrosse, S., & Poitou, C. (2009). Modelling the palaeo-evolution of the geodynamo. *Geophysical Journal International*, *179*(3), 1414–1428. https://doi.org/10.1111/j.1365-246X.2009.04361.x

Aubert, J., Tarduno, J. A., & Johnson, C. L. (2010). Observation and models of the long-term evolution of the Earth's magnetic field. *Space Science Reviews*, *155*, 337–370.

Biggin, A. J., Badejo, S., Hodgson, E., Muxworthy, A. R., Shaw, J., & Dekkers, M. J. (2013). The effect of cooling rate on the intensity of thermoremanent magnetization (TRM) acquired by assemblages of pseudo-single domain, multidomain and interacting single-domain grains. *Geophysical Journal International*, *193*(3), 1239–1249. https://doi.org/10.1093/gji/ggt078

Biggin, A. J., McCormack, A., & Roberts, A. P. (2010). Paleointensity database updated and upgraded. *Eos, Transactions American Geophysical Union*, *91*(2), 15. https://doi.org/10.1029/2010EO020003

Biggin, A. J., & Paterson, G. A. (2014). A new set of qualitative reliability criteria to aid inferences on palaeomagnetic dipole moment variations through geological time. *Frontiers of Earth Science*, *2*, 1–9. https://doi.org/10.3389/feart.2014.00024

Biggin, A. J., Piispa, E. J., Pesonen, L. J., Holme, R., Paterson, G. A., Veikkolanen, T., & Tauxe, L. (2015). Palaeomagnetic field intensity variations suggest Mesoproterozoic inner-core nucleation. *Nature*, *526*, 245–248. https://doi.org/10.1038/nature15523

Biggin, A., Strik, G. H. M. A., & Langereis, C. G. (2009). The intensity of the geomagnetic field in the late-Archaean: New measurements and an analysis of the updated IAGA palaeointensity database. *Earth Planets Space*, *61*, 9–22.

Bispo-Santos, F., D'agrella-Filho, M. S., Trindade, R. I. F., Janikian, L., & Reis, N. J. (2014). Was there SAMBA in Columbia? Palaeomagnetic evidence from 1790 Ma Avanavero mafic sills (northern Amazonian Craton). *Precambrian Research*, *244*, 139–155. https://doi.org/10.1016/j.precamres.2013.11.002

Carvallo, C., Roberts, A. P., Leonhardt, R., Laj, C., Kissel, C., Perrin, M., & Camps, P. (2006). Increasing the efficiency of paleointensity analyses by selection of samples using first-order reversal curve diagrams. *Journal of Geophysical Research*, *111*, B12103. https://doi.org/10.1029/2005JB004126

Celino, K. R., Trindade, R. I. F., & Tohver, E. (2007). LTD-Thellier paleointensity of 1.2 Ga Nova Floresta mafic rocks (Amazon craton). *Geophysical Research Letters*, *34*, L12306. https://doi.org/10.1029/2007GL029550

Coe, R. S. (1967). The determination of paleo-intensities of the Earth's magnetic field with emphasis on mechanisms which could cause non-ideal behavior in Thellier's method. *Journal of Geomagnetism and Geoelectricity*, *19*, 157–179. https://doi.org/10.5636/jgg.19.157

Coe, R. S., Grommé, S., & Mankinen, E. A. (1978). Geomagnetic paleointensities from radiocarbon-dated lava flows on Hawaii and the question of the Pacific nondipole low. *Journal of Geophysical Research*, *83*, 1740–1756. https://doi.org/10.1029/JB083iB04p01740jnmk

de Groot, L. V., Biggin, A. J., Dekkers, M. J., Langereis, C. G., & Herrero-Bervera, E. (2013). Rapid regional perturbations to the recent global geomagnetic decay revealed by a new Hawaiian record. *Nature Communications*, *4*, 2727. https://doi.org/10.1038/ncomms3727

Dekkers, M. J., & Boehnel, H. N. (2006). Reliable absolute palaeointensities independent of magnetic domain state. *Earth and Planetary Science Letters*, *248*, 508–517. https://doi.org/10.1016/j.epsl.2006.05.040

Donadini, F., Elming, S.-Å., Tauxe, L., & Hålenius, U. (2011). Paleointensity determination on a 1.786 Ga old gabbro from Hoting, Central Sweden. *Earth and Planetary Science Letters*, *309*(3–4), 234–248. https://doi.org/10.1016/j.epsl.2011.07.005

Driscoll, P. (2016). Simulating 2 Ga of geodynamo history. *Geophysical Research Letters*, *43*, 5680–5687. https://doi.org/10.1002/2016GL068858

Elming, S. A., Moakhar, M. O., Layer, P., & Donadini, F. (2009). Uplift deduced from remanent magnetization of a proterozoic basic dyke and the baked country rock in the Hoting area, Central Sweden: A palaeomagnetic and 40Ar/39Ar study. *Geophysical Journal International*, *179*, 59–78. https://doi.org/10.1111/j.1365-246X.2009.04265.x

Gattacceca, J., & Rochette, P. (2004). Toward a robust normalized magnetic paleointensity method applied to meteorites. *Earth and Planetary Science Letters*, *227*(3), 377–393. https://doi.org/10.1016/j.epsl.2004.09.013

Haggerty, S. E. (1991). Oxide textures: A mini-altas. In D. H. Lindsley (Ed.), *Reviews in mineralogy. Oxide minerals: Petrologic and magnetic significance* (Vol. 25, pp. 129–137). Washington, DC: Mineralogical Society of America.

Jaeger, J. C. (1968). Cooling and solidification of igneous rocks. In H. H. Hess & A. Poldervaart (Eds.), *Basalts: The Poldervaart treatise on rocks of basaltic composition* (Vol. 2, pp. 503–536). New York, NY: Interscience Publishers.

Kletetschka, G., Wasilewski, P. J., & Taylor, P. P. (2000). Unique thermoremanent magnetization of multidomain sized hematite: Implications for magnetic anomalies. *Earth and Planetary Science Letters*, *176*(3–4), 469–479. https://doi.org/10.1016/S0012-821X(00)00016-9

Kobayashi, K. (1968). Palaeomagnetic determination of the intensity of the geomagnetic field in the Precambrian period. *Physics of the Earth and Planetary Interiors*, *1*, 387–395. https://doi.org/10.1016/0031-9201(68)90035-6

Lacerda-Filho, J. V., Abreu Filho, W., Valente, C. R., Oliveira, C. C., & Albuquerque, M. C. (2004). *Geologia e Recursos Minerais do Estado do Mato Grosso. Texto explicativo dos mapas geológico e de recursos minerais do Estado do Mato Grosso* (Escala1:1.000.000, pp. 235). Convênio CPRM e SICME-MT.

Landeau, M. J., Aubert, J., & Olson, P. (2017). The signature of inner-core nucleation on the geodynamo. *Earth and Planetary Science Letters*, *465*, 193–204. https://doi.org/10.1016/j.epsl.2017.02.004

Muxworthy, A. R. (2010). Revisiting a domain-state independent method of paleointensity determination. *Physics of the Earth and Planetary Interiors*, *179*, 21–31. https://doi.org/10.1016/j.pepi.2010.01.003

Muxworthy, A. R., & Dunlop, D. J. (2002). First-order reversal curve (FORC) diagrams for pseudo-single-domain magnetites at high temperature. *Earth and Planetary Science Letters*, *203*(1), 369–382. https://doi.org/10.1016/S0012-821X(02)00880-4

Muxworthy, A. R., & Heslop, D. (2011). A Preisach method for estimating absolute paleofield intensity under the constraint of using only isothermal measurements: 1. Theoretical framework. *Journal of Geophysical Research*, *116*, B04102. https://doi.org/10.1029/2010JB007844

Muxworthy, A. R., Heslop, D., Paterson, G. A., & Michalk, D. (2011a). A Preisach method for estimating absolute paleofield intensity under the constraint of using only isothermal measurements: 2. Experimental testing. *Journal of Geophysical Research*, *116*, B04103. https://doi.org/10.1029/2010JB007844

Muxworthy, A. R., Ji, X., Ridley, V., Pan, Y., Chang, L., Wang, L., & Roberts, A. P. (2011b). Multi-protocol paleointensity determination from middle Brunhes Chron volcanics, Datong Volcanic Province, China. *Physics of the Earth and Planetary Interiors*, *187*, 188–198. https://doi.org/10.1016/j.pepi.2011.06.005

Paterson, G. A., Heslop, D., & Pan, Y. (2016). The pseudo—Thellier palaeointensity method: New calibration and uncertainty estimates. *Geophysical Journal International*, *207*, 1596–1608. https://doi.org/10.1093/gji/ggw349

Paterson, G. A., Tauxe, L., Biggin, A. J., Shaar, R., & Jonestrask, L. C. (2014). On improving the selection of Thellier-type paleointensity data. *Geochemistry, Geophysics, Geosystems*, *15*, 1180–1192. https://doi.org/10.1002/2013GC005135

Pick, T., & Tauxe, L. (1993). Holocene paleointensities: Thellier experiments on submarine basaltic glass from the East Pacific Rise. *Journal of Geophysical Research*, *98*, 17949–17964. https://doi.org/10.1029/93JB01160

Pozzo, M., Davies, C., Gubbins, D., & Alfe, D. (2012). Thermal and electrical conductivity of iron at Earth's core conditions, *Nature*, *485*(7398), 355–358.

Preisach, F. (1935). Über die magnetische Nachwirkung. *Zeitschrift für Physik*, *94*, 277–302. https://doi.org/10.1007/BF01349418

Reis, N. J., Teixeira, W., Hamilton, M. A., Bispo-Santos, F., Almeida, M. E., & D'agrella-Filho, M. S. (2013). Avanavero mafic magmatism, a late Paleoproterozoic LIP in the Guiana Shield, Amazonian Craton: U–Pb ID-TIMS badde-leyite, geochemical and palaeomagnetic evidence. *Lithos*, *174*, 175–195. https://doi.org/10.1016/j.lithos.2012.10.014

Roberts, A. P., Pike, C. R., & Verosub, K. L. (2000). First-order reversal curve diagrams: A new tool for characterizing the magnetic properties of natural samples. *Journal of Geophysical Research*, *105*, 28461–28475. https://doi.org/10.1029/2000JB900326

Santos, J. O. S., Potter, P. E., Reis, N. J., Hartmann, L. A., Fletcher, I. R., & McNaughton, N. J. (2003). Age, source, and regional stratigraphy of the Roraima Supergroup and Roraima-like outliers in northern South America based on U–Pb geochronology. *Bulletin of the Geological Society of America*, *3*, 31–348. https://doi.org/10.1130/0016-7606(2003)115<0331:ASARSO>2.0.CO;2

Shaar, R., & Tauxe, L. (2013). Thellier GUI: An integrated tool for analyzing paleointensity data from Thellier-type experiments. *Geochemistry, Geophysics, Geosystems*, *14*, 677–692. https://doi.org/10.1002/ggge.20062

Shaw, J. (1974). A new method of determining the magnitude of the palaeomagnetic field, application to five historic lavas and five archaeological samples. *Geophysical Journal of the Royal Astronomical Society*, *39*, 133–141. https://doi.org/10.1111/j.1365-246X.1974.tb05443.x

Shcherbakova, V. V., Shcherbakov, V. P., Didenko, A. N., & Vinogradov, Y. K. (2006). Determination of the paleointensity in the early Proterozoic from Garanitoids of the Shumikhinskii Complex of the Siberian Craton. *Izvestiya, Physics of the Solid Earth*, *42*, 521–529. https://doi.org/10.1134/S1069351306060097

Shcherbakova, V. V., Shcherbakov, V. P., Zhidkov, G. V., & Lubnina, N. V. (2014). Paleointensity determinations on rocks from Palaeoproterozoic dykes from the Kaapvaal Craton (South Africa). *Geophysical Journal International*, *197*(3), 1371–1381. https://doi.org/10.1093/gji/ggu098

Schwarz, E. J., & Symons, D. T. A. (1969). Geomagnetic intensity between 100 million and 2500 million years ago. *Physics of the Earth and Planetary Interiors*, *2*, 11–18. https://doi.org/10.1016/0031-9201(69)90014-4

Schwarz, E. J., & Symons, D. T. A. (1970). Palaeomagnetic field intensity during cooling of the Sudbury irruptive 1700 million years ago. *Journal of Geophysical Research*, *74*, 6631–6640. https://doi.org/10.1029/JB075i032p06631

Smirnov, A. V., & Tarduno, J. A. (2005). Thermochemical remanent magnetization in Precambrian rocks: Are we sure the geomagnetic field was weak? *Journal of Geophysical Research*, *110*, B06103. https://doi.org/10.1029/2004JB003445

Smirnov, A. V., Tarduno, J. A., Kulakov, E. V., McEnroe, S. A., & Bono, R. K. (2016). Paleointensity, core thermal conductivity and the unknown age of the inner core. *Geophysical Journal International*, *205*, 1190–1195. https://doi.org/10.1093/gji/ggw080

Smirnov, A. V., Tarduno, J. A., & Pisakin, B. N. (2003). Paleointensity of the early geodynamo (2.45 Ga) as recorded in Karelia: A single-crystal approach. *Geology*, *31*(5), 415–418. https://doi.org/10.1130/0091-7613(2003)031<0415:POTEGG>2.0.CO;2

Tassinari, C. C. G., & Macambira, M. J. B. (1999). Geochronological provinces of the Amazonian Craton. *Episodes*, *22*, 174–182.

Tauxe, L., & Staudigel, H. (2004). Strength of the geomagnetic field in the Cretaceous Normal Superchron: New data from submarine basaltic glass of the Troodos Ophiolite. *Geochemistry, Geophysics, Geosystems*, *5*, Q02H06. https://doi.org/10.1029/2003GC000635

Tauxe, L., & Yamazaki, T. (2007). Paleointensities. In M. Kono (Ed.) *Treatise on geophysics* (Vol. 5, pp. 509–563). New York, NY: Elsevier.

Thellier, E., & Thellier, O. (1959). Sur l'intensite du champ magnetique terrestre dans le passe historique et geologique. *Annals of Géophysics*, *15*, 275–376.

Thomas, N. (1993). An integrated rock magnetic approach to the selection or rejection of ancient basalt samples for paleointensity experiments. *Physics Earth and Planetary Interiors*, *75*, 329–342. https://doi.org/10.1016/0031-9201(93)90008-W

Valet, J. P., Herrero-Bervera, E., & Carlut, J. (2010). A selective procedure for absolute paleointensity in lava flows. *Geophysical Research Letters*, *37*, L16308. https://doi.org/10.1029/2010GL044100

Walton, D., Share, J., Rolph, T. C., & Shaw, J. (1993). Microwave magnetisation. *Geophysical Research Letters*, *20*(2), 109–111. https://doi.org/10.1029/92GL02782

Yamamoto, Y., Tsunakawa, H., & Shibuya, H. (2003). Paleointensity study of the Hawaiian 1960 lava: Implications for possible causes of erroneously high intensities. *Geophysical Journal International*, *153*, 263–276. https://doi.org/10.1046/j.1365-246X.2003.01909.x

Ziegler, L. B., & Stegman, D. R. (2013). Implications of a long-lived basal magma ocean in generating Earth's ancient magnetic field. *Geochemistry, Geophysics, Geosystems*, *14*, 4735–4742. https://doi.org/10.1002/2013GC005001